

Conductive $\text{LaAlO}_3/\text{SrTiO}_3$ and $\text{LaGaO}_3/\text{SrTiO}_3$ interfaces at high oxygen pressure in the shock-wave regime of pulsed laser deposition

C. Aruta,* S. Amoruso, G. Ausanio, R. Bruzzese, E. Di Gennaro, M. Lanzano,
F. Miletto Granozio, Muhammad Riaz, U. Scotti di Uccio, and X. Wang
CNR-SPIN and Dipartimento di Scienze Fisiche,
Complesso Universitario di Monte Sant'Angelo, Via Cintia, I-80125 Napoli, Italy
(Dated: February 22, 2019)

Pulsed laser deposition of $\text{LaAlO}_3/\text{SrTiO}_3$ and $\text{LaGaO}_3/\text{SrTiO}_3$ conducting interfaces at an oxygen background pressure of $\approx 10^{-1}$ mbar, well above the previously reported limit for the conductivity, is investigated. In this regime, the shock wave-like propagation of the plume close to the substrate is able to provide enough plume internal energy to promote surface diffusion and favor two-dimensional layer-by-layer growth of conductive interfaces. The high oxygen pressure of 10^{-1} mbar promotes the correct oxidation of the samples, so that the influence of oxygen defects on the observed interfacial conductivity is expected to be drastically reduced.

The discovery of a two-dimensional electron gas (2DEG) at the interface between a LaAlO_3 (LAO) film and a TiO_2 -terminated SrTiO_3 (STO) substrate by Ohtomo et al. [1] immediately attracted a tremendous interest in the scientific community. Since then, a widespread, experimental and theoretical activity, devoted to the investigation of LAO/STO interfaces and of other systems that may potentially share similar properties, started. Recently, $\text{LaGaO}_3/\text{SrTiO}_3$ (LGO/STO) interfaces were also shown to host a 2DEG [2, 3]. In spite of the huge efforts, the debate on the involved mechanisms is still open and the origin of the interface metallic behavior is still under intensive investigation. A model based on an electronic reconstruction at the interface (the “polar-catastrophe”) assumes the transfer of electrons from the free surface of LAO into the interface region [4], allowing the release of part of the electrostatic energy associated with the polar state of LAO. Such model correctly predicts that LAO must be thicker than 3-4 unit cells (uc) to allow for conductivity, and that growth on SrO-terminated STO does not provide a conducting state. A similar explanation was also proposed for LGO/STO on the base of first principle calculations [3]. In addition to intrinsic interfacial reconstruction, growth related extrinsic factors are also considered as possible sources of the interface conductivity. Among them, oxygen vacancies and cation substitution are possible chemical defects occurring during growth.

These hetero-interfaces are usually elaborated by pulsed laser deposition (PLD) in an oxygen atmosphere. It is generally considered that layer-by-layer growth and conductive interfaces occur only when the oxygen pressure is between 10^{-6} - 10^{-3} mbar[5–7]. Unfortunately, such low pressures have two drawbacks. First, STO might be doped by oxygen vacancies, which act as donors [5–7]. Even though post annealing treatments decrease the amount of such vacancies, doubts remain that the conductivity of the interface is due to local oxygen deficiency. Second, at low pressure the kinetic energy of cations in the ablation plume is high. It was then argued that some

cation intermixing at the interface may take place due to La subplantation [6, 8–10], resulting in the formation of a $\text{La}_x\text{Sr}_{1-x}\text{TiO}_3$ conductive layer. However, a recent study indicates that the relevance of such a mechanism is considerably reduced at an oxygen pressure of 5×10^{-2} mbar [11]. Since oxygen vacancies and interface disorder can be drastically reduced by an oxygen pressure increase during deposition, it is motivating to investigate if high quality, conducting oxide hetero-interfaces can be deposited at high ($p \approx 10^{-1}$ mbar) oxygen pressure.

Here we report on conducting interfaces of LAO/STO and LGO/STO grown at an oxygen pressure of $\approx 10^{-1}$ mbar, evidencing the ablation plume condition leading to this achievement. Our findings clearly indicate the beneficial role of the shock-wave (SW) regime on the interfacial conductivity properties at this high background pressure. As demonstrated in this study, this condition leads to the arrival on the STO substrate of a plume characterized by a large oxidation and a considerable amount of excited species of rather low kinetic energy.

LAO and LGO films were grown by PLD on a TiO_2 -terminated (001) STO substrate. A KrF excimer laser beam (248 nm, 25 ns duration full width half maximum) was focused on a stoichiometric target placed at a distance of about 30 mm from the STO substrate. The laser spot-size on target, and fluence were 1.5×10^{-2} cm^2 and 2.5 J/cm^2 , respectively. The films were grown at a substrate temperature of 800°C and at an oxygen pressure of 10^{-1} mbar. The growth process was monitored by in-situ high pressure reflection high energy electron diffraction (RHEED). Moreover, the ablation plume was investigated by fast photography and space-resolved optical emission spectroscopy [12–14]. Oscillations of the RHEED diffracted pattern intensity registered during the growth of a 12 uc thick LGO film are shown in Fig. 1(a), as an example of the growth process at 10^{-1} mbar in our experimental conditions. Similar RHEED oscillations were also observed at lower oxygen pressure [2]. On the base of the clear 2D RHEED pattern at the end of deposition, as shown on the top of Fig.1(a), we rule

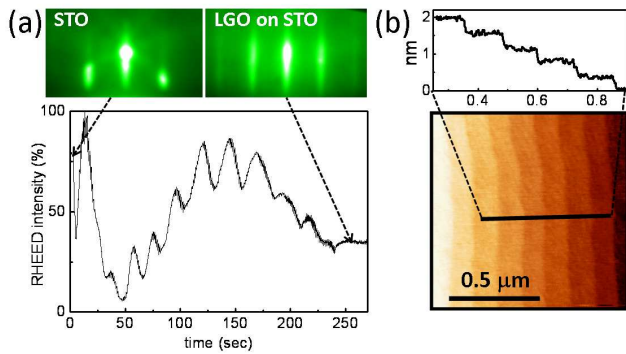


Figure 1: (Color online) (a) RHEED intensity monitoring of LGO on STO at $p=10^{-1}$ mbar. STO RHEED pattern before the deposition and final RHEED pattern after growth of 12 unit cells of LGO are also shown on the top. (b) AFM height image of 12 uc LGO at $p=10^{-1}$ mbar. The cross section corresponding to the straight line in the image is reported on the top.

out significant variation of the surface ordering during the growth process. RHEED oscillations and the final 2D RHEED pattern were also observed for LAO growth [15]. Fig. 1(b) reports an atomic force microscopy (AFM) image, demonstrating that the LGO layer surface is characterized by high flatness. Terraces separated by 1 uc steps are clearly observed in the profile reported on the top of Fig.1(b). Even though one cannot completely rule out the possibility of nanoscale roughness on portions of the terraces due to the limited sharpness of the AFM tip, the fairly well-defined terraces in concert with the RHEED oscillations suggest that the 2D growth mode is dominant. These results show that, even at a pressure of $\approx 10^{-1}$ mbar, deposition conditions can be found where the PLD growth proceeds in an essential layer-by-layer mode. Similar results were also observed for LAO, although terraces edges were not as sharp, and obtaining a flat sample turned out to be more critical. According to the mechanisms proposed by Willmott *et al.* [16], stable 2D growth of a complex metal-oxide is typically achieved at an oxygen pressure below 10^{-2} mbar. In fact, at low pressure the ablated species reach the substrate with a maximum kinetic energy KE_m of several tens eV [15]. These energetic particles break-up the small nuclei that are formed on the growing front of the film; the crystallization process is then promoted by the enhanced surface diffusion of adatoms [16]. At 10^{-1} mbar, instead, KE_m reduces to tenths of eV [15]. As a consequence, the achievement of a 2D growth regime of LAO and LGO on STO at high oxygen pressure is particularly interesting.

The temperature-dependent sheet resistance of 12 uc thick LGO/STO and LAO/STO samples grown at an oxygen pressure of $\approx 10^{-1}$ mbar was analyzed, and the results are reported in Fig. 2. Both samples exhibit

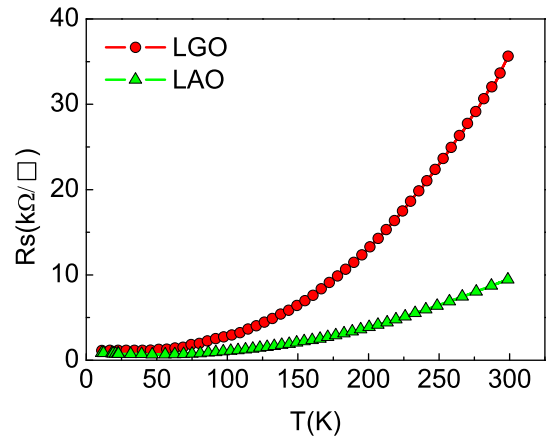


Figure 2: Temperature dependence of the sheet resistance of LGO/STO and LAO/STO interfaces grown at oxygen pressure of 10^{-1} mbar.

a clear metallic conducting behaviour, and the values of the resistance are similar to those obtained at low pressure [2]. Consequently, in our case one can suppose that both the La-subplantation and STO oxygen vacancies mechanisms, usually considered at lower pressure, are of minor importance. Nevertheless, it is worth stressing that also other extrinsic mechanisms, such as (i) oxygen diffusion from STO to the growing film [17], and (ii) redox reactions on the surface of STO [18], have been recently suggested. In Ref.[17], LAO films were deposited at low pressure ($\approx 10^{-5}$ mbar), a condition where an insufficient oxidation of the LAO overlayer is expected. In our case, the higher deposition pressure leads to a much larger oxidation of the plume species reaching the substrate [15]. The better oxidation of the LAO overlayer, then, suggests that the diffusion of oxygen from the STO substrate, to compensate the insufficient oxidation of growing overlayer, can be considered negligible. In Ref.[18], it is proposed that in LAO/STO the redox reaction of Al, depositing on the TiO_2 substrate surface, leads to the generation of oxygen vacancies. This is explained in terms of standard heat of formation (per mole of oxygen), ΔH_f^O . In fact, in case of Al and Ti, the relation $|\Delta H_f^O(Al)| > |\Delta H_f^O(Ti)|$ holds true [19]. Nevertheless, we obtained a conductive interface also in the case of the LGO/STO interface. Since $|\Delta H_f^O(Ga)| < |\Delta H_f^O(Ti)|$ [20], the redox mechanism suggested in Ref.[18] might not be effective in our case.

In an attempt to clarify the differences between the two growth regimes of low ($p \leq 10^{-2}$ mbar) and high pressure ($p \approx 10^{-1}$ mbar), we studied the changes in the ablation plume by fast photography. Single-shot, fast images of the LGO plume emission taken by intensified-charge-coupled device (ICCD) [12–14] at 10^{-3} and 10^{-1} mbar, at two succeeding delays τ after the laser pulse, are reported in Fig. 3 (a). The images at 10^{-3} mbar are rep-

representative of the low-pressure deposition condition, usually employed in PLD interface deposition, while those at 10^{-1} mbar allow evidencing the variation induced on the plume in the new regime here explored. The image intensity is multiplied by an appropriate factor, reported in parenthesis in the bottom-left corner of each panel, in order to get rid of the progressive reduction of the intensity with τ as a consequence of the plume expansion, and to facilitate the comparison. The images of Fig. 3(a) show a significant influence of oxygen pressure on plume propagation dynamics, intensity and shape which will eventually affect growth dynamics and film characteristics. The plasma plume propagation in the ambient gas is usually analyzed by using position-time plots of the leading edge of the plume emission along the normal to the target surface [12–14]. The plume front position R is defined as the distance at which the integral of the emission intensity attains a value equal to 95% of the total emission along the direction, z , normal to the target surface [14]. Fig. 3 (b) reports the time evolution of the plume front position, R , along z [12–14], at three different oxygen pressures. The curve obtained at $p \approx 1$ mbar is reported to show a clear example of plume temporal dynamics evolving from free expansion, at early delay, to plume braking and, eventually, to plume stopping, at longer delays, over a distance of few centimeters [14, 21–23]. In particular, from Fig. 3(b) we noticed that the plume propagation dynamics follows a free-expansion ($R \propto \tau$) at pressure $p \leq 2 \times 10^{-2}$ mbar. The corresponding images of Fig. 3(a) at 10^{-3} mbar show a significant decrease of the plume intensity with τ , due to its progressive decrease of density and temperature. At higher pressures, the plume-background gas interaction causes plume deceleration, together with SW formation [14, 21–23]. A particularly interesting feature, central to our analysis, can be observed in the curve corresponding to plume expansion at $p=10^{-1}$ mbar (circles, red curve). Starting from about $3 \mu\text{s}$, a clear deviation from the linear temporal dependence characterizing the free-plume expansion regime is observed: in fact, a SW-like propagation dynamics ($R \propto \tau^{2/5}$, red curve) starts. A similar dynamics (blue curve) is observed at $p=1$ mbar, but at earlier delays τ , due to the distance-related-pressure influence of the ambient gas on the propagation dynamics and energetic state of the expanding plume [14, 22, 24, 25]. As a consequence of the plume interaction with the background gas, the images at 10^{-1} mbar in Fig. 3(a) show a much more intense plume emission, indicating the formation of a large number of excited species in this condition. These excited species are mainly located at the plume front and directly impact on the STO substrate, thus influencing the film growth. At the still larger pressure of ≈ 1 mbar, SW is followed by a further slow-down until the plume eventually reaches a stopping regime at longer delays. In this last case, the plume species can reach the substrate at a distance of 30 mm only through

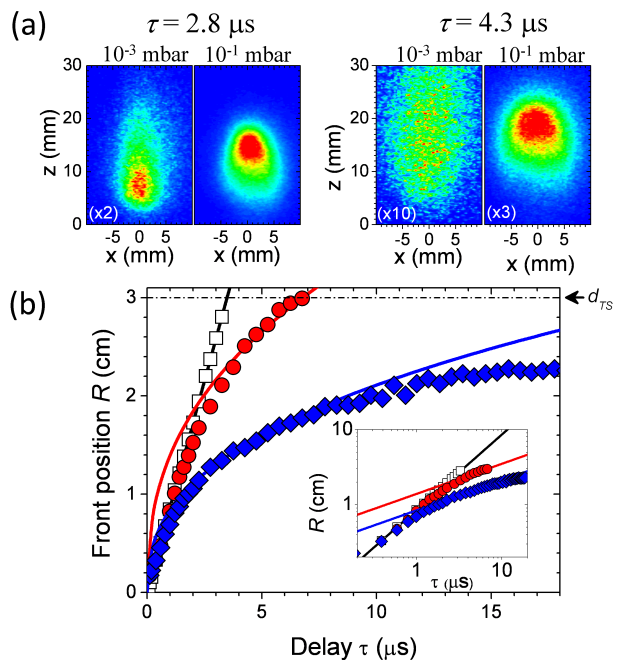


Figure 3: ((Color online) (a) 2D single shot images of the LGO plume emission at 10^{-3} and 10^{-1} mbar for two different delays τ after the laser pulses. The plume propagation direction is along the z -axis, and $z=0$ marks the position of the target surface, while the x -axis is parallel to the target surface. (b) Position-time R - τ plots of the plume front at different pressure p : $p \leq 2 \times 10^{-2}$ mbar (squares), $p=10^{-1}$ mbar (circles) and $p=1$ mbar (diamonds). The solid lines are the calculated behaviors for free-expansion at $p \leq 2 \times 10^{-2}$ mbar and SW-like regime at $p=10^{-1}$ and 1 mbar. The dashed curve indicate the target-substrate distance $d_{TS}=3$ cm. The inset show the log-log plot of the plume dynamics data.

diffusion into the background gas [26]. This, in turn, evidences the critical dependence of the plume properties on the oxygen pressure and distance from the target surface, which can finally affect the quality of the deposited films, as discussed hereafter.

As a consequence of the above observations, we can conclude that in case of LGO and LAO films grown at $p \approx 10^{-1}$ mbar, the deposition process takes place in rather peculiar conditions. In fact, the SW regime takes place when the plume front has reached distances comparable to the target-substrate distance (see Fig. 3(b)), an experimental condition which determines a higher internal energy of the plume during the growth process [22, 25]. In particular, a much larger amount of excited plume species reaches the substrate in such a condition. The upper electronic levels of these excited species are at 2-3 eV above the ground state. This internal excitation energy is eventually supplied to the growing film during deposition [27]. This energy is comparable with the maximum surface diffusion barrier energy at high coverage reported in ref. [16] and, when released to the

growing film, can promote surface diffusion, thus resulting in the observed 2D growth. Thus, appropriate tuning of the experimental parameters allows selecting a condition where the SW-like regime facilitates the deposition of conducting interfaces even at an oxygen pressure of $\approx 10^{-1}$ mbar. It is, however, worth to mention that at high pressure the relative alignment of plume and substrate, as well as the target-to-substrate distance, become critical parameters of the deposition experiment. As an example, in similar experimental conditions a slightly longer target-to-substrate distance resulted in the deposition of insulating samples [15], thus indicating a rather narrow range for the optimal values of the processing parameters leading to conductive interfaces at high pressure. This critical behavior can be ascribed to the fact that when the plume is braked and partially confined by high oxygen background pressures, the final plume characteristics at the substrate distance are significantly affected by even small changes of the ablation conditions.

In conclusion, we used simultaneous analysis of the plume dynamics and film growth to determine the experimental conditions suitable for deposition of conducting oxide hetero-interfaces in a situation where an optimal oxidation of the film can be also achieved. This is attained by using an oxygen pressure of $\approx 10^{-1}$ mbar and locating the substrate at a position close to where SW regime of the plume propagation takes place in our experimental conditions. In this situation the interfacial conducting properties should be free from extensive oxygen defects contribution. The chance of releasing the constraint of low oxygen pressure growth can allow deeper understanding of the role of the various mechanisms contributing to interfaces conductivity. This opens new perspectives in the comprehension of the subtle mechanisms underlying the formation of the electron gas developing at polar/non-polar interfaces, and, more generally, of the growth process of well oxygenated and well ordered oxide interfaces, where the intrinsic interfacial reconstruction has to be disentangled by extrinsic growth related effects.

The research leading to these results has received funding from European Union Seventh Framework Programme (FP7/2007-2013) under grant agreement N. 264098 - MAMA, and from the Italian Ministry of Education, University and Research (MIUR) under Grant Agreement PRIN 2008 - 2DEG FOXI.

* Electronic address: carmela.aruta@spin.cnr.it

- [1] A.Ohtomo and H. Y. Hwang, *Nature* **427**, 423 (2004); **441**, 120 (2006)
- [2] P. Perna, D. Maccariello, M. Radovic, U. Scotti di Uccio, I. Pallecchi, M. Codda, D. Marré, C. Cantoni, J. Gazquez, M. Varela, S. Pennycook, and F. Miletto Granozio, *Appl. Phys. Lett.* **97**, 152111 (2010)
- [3] S. Nazir, N. Singh, and U. Schwingenschlögl, *Appl. Phys. Lett.* **98**, 262104 (2011)
- [4] N. Nakagawa, H. Y. Hwang and D. A. Muller, *Nat. Mater.* **5** 204 (2006)
- [5] M. Huijben, A. Brinkman, G. Koster, G. Rijnders, H. Hilgenkamp, and D. H. A. Blank, *Adv. Mater.* **21**, 1665 (2009)
- [6] J.-L. Maurice, G. Herranz, C. Colliex, I. Devos, C. Carrétéro, A. Barthélémy, K. Bouzehouane, S. Fusil, D. Imhoff, É. Jacquet, F. Jomard, D. Ballutaud, M. Basletic, *Europhys. Lett.* **82**, 17003 (2008).
- [7] A. Kalabukhov, R. Gunnarsson, J. Brjesson, E. Olsson, T. Claeson, D. Winkler, *Phys. Rev. B* **75**, R121404 (2007)
- [8] P.R. Willmott, S.A. Pauli, R. Herger, C. M. Schlepütz, D. Kumah, C. Cionca and Y. Yacoby, *Phys. Rev. Lett.* **99**, 155502 (2007).
- [9] S.A. Chambers, M.H. Engelhard, V. Shutthanandan, Z. Zhu, T.C. Droubay, L. Qiao, P.V. Sushko, T. Feng, H.D. Lee, T. Gustafsson, E. Garfunkel, A.B. Shah, J.-M. Zuo, Q.M. Ramasse, *Surf. Sci. Rep.* **65**, 317 (2010)
- [10] C. L. Jia, S. B. Mi, M. Faley, U. Poppe, J. Schubert and K. Urban *Phys. Rev. B* **79**, R081405 (2009).
- [11] A. Kalabukhov, Yu. A. Boikov, I.T.Serenkov, V.I.Sakharov, J.Börjesson, N. Ljustina, E. Olsson, D.Winkler and T. Claeson, *Eur. Phys. Lett.* **93** 37001 (2011)
- [12] D. B. Geohegan, *Appl. Phys. Lett.* **67**, 197 (1995)
- [13] S. S. Harilal, C. V. Bindhu, M. S. Tillack, F. Najmabadi, A. C. Gaeris, *J. Appl. Phys.* **93**, 2380 (2003).
- [14] A. Sambri, S. Amoruso, X. Wang, F. Miletto Granozio, R. Bruzzese, *J. Appl. Phys.* **104**, 053304 (2008).
- [15] C. Aruta, S. Amoruso, R. Bruzzese, X. Wang, D. Maccariello, F. Miletto Granozio, and U. Scotti di Uccio *Appl. Phys. Lett.* **97**, 252105 (2010)
- [16] P. R. Willmott, R. Herger, C.M. Schlepütz, D. Martoccia, and B. D. Patterson, *Phys. Rev. Lett.* **96**, 176102 (2006)
- [17] W. Schneider, M. Esposito, I. Marozau, K. Conder, M. Doebeli, Yi Hu, M. Mallepell, A. Wokaun, and T. Lippert, *Appl. Phys. Lett.* **97**, 192107 (2010)
- [18] Y. Chen, N. Pryds, J. E. Kleibeuker, G. Koster, J. Sun, E. Stamate, B. Shen, G. Rijnders, and S. Linderöth, *Nano Letters* **11**, 3774 (2011)
- [19] C.T. Campbell, *Surf. Sci. Rep.* **27**, 111 (1997)
- [20] *Handbook of Chemistry and Physics*, edited by D. R. Lide (CRC, Boca Raton, 1993).
- [21] A. Sambri, S. Amoruso, X. Wang, M. Radovic, F. Miletto Granozio, R. Bruzzese, *Appl. Phys. Lett.* **91**, 151501 (2007)
- [22] N. Arnold, J. Gruber, and J. Heitz, *Appl. Phys. A* **69**, S87 (1999)
- [23] S. Amoruso, J. Schou, J. G. Lunney, *Appl. Phys. A* **92**, 907 (2008)
- [24] S. Amoruso, C. Aruta, R. Bruzzese, D. Maccariello, L. Maritato, F. Miletto Granozio, P. Orgiani, U. Scotti di Uccio, and X. Wang, *J. Appl. Phys.* **108**, 043302 (2010).
- [25] S. Amoruso, J. Schou, and J. G. Lunney, *Appl. Phys. A* **101** 209 (2010)
- [26] S. Amoruso, B. Toftmann, J. Schou, *Phys. Rev. E* **69**, 056403(2004)
- [27] A. Anders, *Appl. Phys. Lett* **80**, 1100 (2002)